Determination of Porosity-A Casting Defect Occurrence in Green-Sand Casting of Al-Si5-Cu3 by the Taguchi Method

Chirag Jadav[1]*, Shailesh Patel[2]

Ph.D. Scholar, Faculty of Engineering & Technology, Sankalchand Patel University, Visnagar, Gujarat, India[1]
Assistant Professor, Basic Engineering and Applied Sciences Department, College of Agricultural Engineering & Technology, Anand Agricultural University, Godhra, Gujarat, India[2]

chiragvjadav@gmail.com*, skpatel.sspc@spu.ac.in

Abstract: Porosity is a significant concern in Al-Si_5-Cu_3, aluminum alloy casting, tending to considerably more scrap outcomes and limiting parts use in critical applications due to porosity. This defect is directly relevant to the manufacturing process thus its occurrence is closely tied to green sand-casting process parameters. Here implementing of Taguchi method offers substantial porosity reduction mapping during casting with different input parameters. A combined experiment has been carried out using Taguchi's L27 orthogonal array (OA) to study the main effect and interaction effect of all five parameters. In a thick-walled sample casting, pouring temperature and pouring time significantly affect porosity reduction. Pouring temperature having F-Value of 8.47 and a low P-Value of 0.003, and F-Value of 5.76 and a corresponding P-Value of 0.013 of the pouring time, indicating its influential role in explaining the variation in both Average Porosity and S/N Ratio Degassing time and mould temperatures have marginal effects, while crucible volume hold minimally influences porosity. The interaction between pouring temperature, pouring time, and crucible volume in green sand casting significantly impacts the output, indicating significance influential factors for porosity occurrence, as their p-values are below 0.05 or very close to it. Assessing the anticipated enhancements in quality and the potential for cost savings based on optimal parameters forecasts a decrease in porosity and minimized losses prior to conducting experimental trials.

Keywords: Taguchi approach, Orthogonal Array (OA), Green-sand casting process, Aluminum casting porosity, ANOVA

I. INTRODUCTION

Since the late 1950s, Dr. Genichi Taguchi has pioneered numerous innovative statistical tools and quality improvement concepts rooted in the principles of experimental design [3,8,9]. His methodology revolves around enhancing product and process quality by: (a) crafting designs resilient to environmental variations, (b) developing robust systems capable of withstanding component discrepancies, and (c) minimizing deviations from desired target values.

Dr. Taguchi's philosophy delineates three pivotal stages in process development [12]: (a) System Design: where engineers utilize scientific and engineering tenets to establish the fundamental configuration, (b) Parameter Design: involving the determination of specific parameter values, and (c) Tolerance Design: focusing on specifying optimal tolerances for these parameters [3,9,12,16].

Numerous documented instances across the foundry industry underscore the efficacy of Taguchi's methods in mitigating the adverse effects of uncontrollable process variables on casting quality [18]. Green-sand casting, a prevalent manufacturing technique for producing intricate parts, presents a multitude of parameters influencing casting quality [22]. While some parameters are within control, others act as noise factors. Hence, green-sand casting sector emerges as an ideal arena for implementing Taguchi's test methodologies to foster continuous and swift quality enhancements.

Implementation of the Taguchi technique in the green sand-casting process can yield significant reductions in porosity formation. Despite extensive research, design, and development efforts, the persistent challenge of porosity in pressure green sand castings remains. The escalating complexity of castings demanded by industry renders complete elimination of porosity virtually impossible. However, optimization techniques for casting parameters can effectively confine porosity to non-critical areas.

Porosity formation in aluminum alloys is particularly problematic, as it not only compromises the mechanical properties of castings but also adversely affects their machinability and surface properties. Two primary sources contribute to porosity: solidification shrinkage and the release of dissolved gases. Shrinkage porosity correlates with thermal and solidification parameters, while gas porosity is directly influenced by pouring time and method, moisture evaporation from the cavity or

mould, and the release of hydrocarbons from burning off oil-based lubricants.

In green sand castings, it is widely recognized that neither gas solubility nor shrinkage significantly contribute to porosity. Instead, the most significant source stems from entrapped air within the molten metal during pouring into the mould cavity [22,23].

The objective of this paper is to explore the influence of process parameters on porosity formation in green-sand casting, with the aim of enhancing casting quality. The following steps outline the approach taken to achieve this goal:

1. Define casting porosity as the quality characteristic to be improved. In the context of green-sand casting, the objective is to minimize casting porosity, considering it as "the smaller, the better," while mitigating the impact of uncontrollable parameters.
2. Identify the most influential green-sand casting parameters contributing to porosity variation.
3. Conduct the green-sand casting process according to the experimental conditions prescribed by the selected orthogonal array (OA) and parameter levels and collect relevant data.
4. Perform data analysis, including the generation of an analysis of variance (ANOVA) table to ascertain the statistical significance of the parameters. Response graphs are generated to identify the optimal levels for each parameter.
5. Determine the optimal settings for the control parameters based on the analysis.
6. Forecast the expected porosity formation resulting from the optimal parameter levels.
7. Estimate the potential cost savings achievable with the implementation of the optimal parameter settings.

II. PARAMETER DESIGN

In the green sand-casting process, molten metal is poured into rigid mould cavities, with three key factors predominantly influencing its efficacy: pouring velocity (whether it's fast or slow), pouring rate, and pouring time. Preheating the mould to a specific temperature is imperative to prevent shrinkage or gas porosity defects. Additionally, the success of green-sand casting hinges on various parameters such as the volume held in the crucible, the degassing of both the molten metal and the mould, and the chosen solidification method.

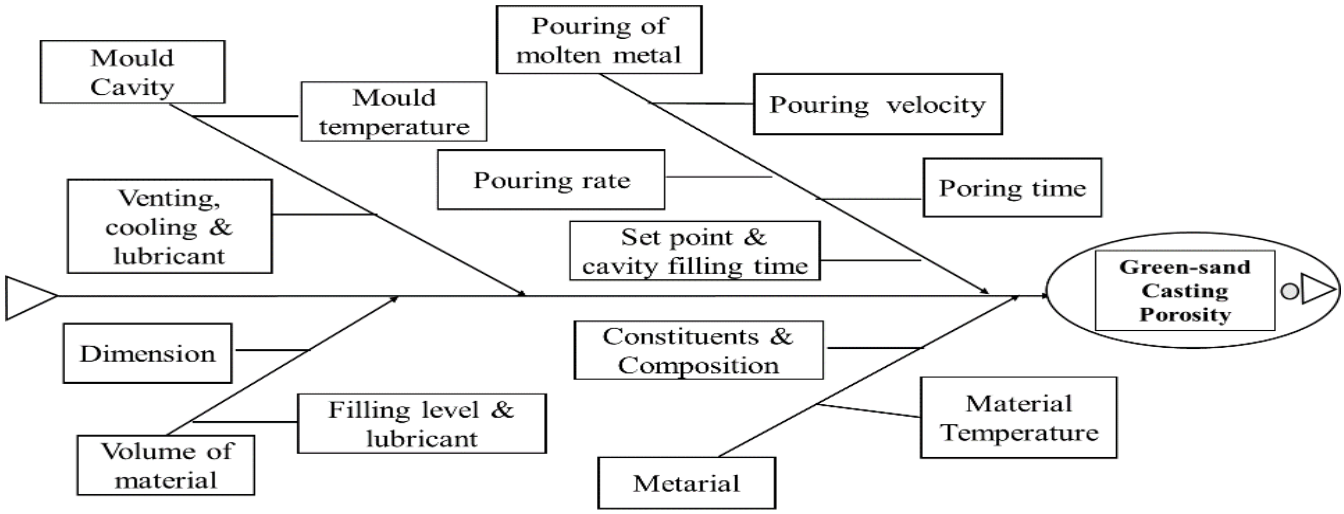

Figure:1 Fishbone diagram for the casting parameters

Porosity formation in green sand-casting stems from a multitude of factors. A Fishbone diagram (Fig. 1) was devised to pinpoint the casting process parameters that could potentially influence casting porosity. Pouring temperature (factor A), pouring time (factor B), volume held in the crucible (factor C), degassing time (factor D), and mould temperature (factor E) emerged as the most critical factors in the experimental design. Throughout the experimentation, other parameters remained constant.

The pouring temperature ranged from 710 to 740°C, degassing time varied between 10 and 15 minutes, the volume held in the crucible ranged from 100 to 400 kg, pouring time was maintained between 1.4 and 3.8 m/s, and mould temperature spanned from 180 to 270°C. Table I outlines the selected casting process parameters alongside their respective ranges.

Experience demonstrates that the intricate nature of casting process parameters becomes evident only when explored across multiple levels. Thus, each parameter was meticulously scrutinized across three levels. Existing literature underscores the significance of analysing the holding furnace temperature in tandem with the temperature applied (*A X B*), as well as in conjunction with the volume held in the crucible (*A X C*), and the pouring time in combination with the volume held in the crucible (*B X C*),

in influencing porosity formation during casting. Consequently, the interplay among these parameters was deemed essential for thorough investigation.

Table I
CASING PARAMETERS AND THEIR RANGES

Parameter designation	Process Parameter	Process Parameter Range	Level 1	Level 2	Level 3
A	Pouring temperature (^{0}C)	710-740	710	725	740
B	Pouring time (min)	1.4-3.8	1.4	2.6	3.8
C	Volume hold in crucible (kg)	100-400	100	250	400
D	Degassing time (s)	10-15	10	12	15
E	Mould temperature (^{0}C)	180-270	180	225	270

A. TAGUCHI DESING

Design Summary		Interactions
Taguchi Array	L_{27}(3^5)	AB
Factors:	5	AC
Runs:	27	BC

Table II
L_{27} OA ASSIGNED PROCESS PARAMETER AND INTERACTION.

Run	*A*	*B*	*A X B*	*A X B²*	*C*	*A X C*	*A X C²*	*B X C*	*D*	*E*	*B X C²*
1	1	1	1	1	1	1	1	1	1	1	1
2	1	1	1	1	2	2	2	2	2	2	2
3	1	1	1	1	3	3	3	3	3	3	3
4	1	2	2	2	1	1	1	2	2	2	3
5	1	2	2	2	2	2	2	3	3	3	1
6	1	2	2	2	3	3	3	1	1	1	2
7	1	3	3	3	1	1	1	3	3	3	2
8	1	3	3	3	2	2	2	1	1	1	3
9	1	3	3	3	3	3	3	2	2	2	1
10	2	1	2	3	1	2	3	1	2	3	1
11	2	1	2	3	2	3	1	2	3	1	2
12	2	1	2	3	3	1	2	3	1	2	3
13	2	2	3	1	1	2	3	2	3	1	3
14	2	2	3	1	2	3	1	3	1	2	1
15	2	2	3	1	3	1	2	1	2	3	2
16	2	3	1	2	1	2	3	3	1	2	2
17	2	3	1	2	2	3	1	1	2	3	3
18	2	3	1	2	3	1	2	2	3	1	1
19	3	1	3	2	1	3	2	1	3	2	1
20	3	1	3	2	2	1	3	2	1	3	2
21	3	1	3	2	3	2	1	3	2	1	3
22	3	2	1	3	1	3	2	2	1	3	3
23	3	2	1	3	2	1	3	3	2	1	1
24	3	2	1	3	3	2	1	1	3	2	2
25	3	3	2	1	1	3	2	3	2	1	2
26	3	3	2	1	2	1	3	1	3	2	3
27	3	3	2	1	3	2	1	2	1	3	1

The total degree of freedom (*DOF*) required for five factors, each spanning three levels along with three interactions, amounts to 22. In this study, a three-level orthogonal array (*OA*) comprising 27 experimental runs (resulting in *DOF* = 27-1 = 26) has been chosen. Given that each interaction encompasses four *DOF*, a total of six columns (two columns per interaction) are necessary to represent these interactions accurately. Utilizing a triangular table for the three-level OA facilitates the identification of interacting columns within the L_{27} *OA*, allowing parameters to be systematically assigned to columns [16,23]. Table II provides a comprehensive breakdown of the assignment of casting process parameters (denoted as A to E) and parameter interactions (such as $A \times B$, $A \times B^2$, $A \times C$, $A \times C^2$, $B \times C$, and $B \times C^2$) across columns.

III. EXPERIMENT

The use of high-performance and high-accuracy equipment that would be able to secure the correct measurement of green-sand casting parameter values and react in time for the necessary corrective actions was required in the experimental procedure. Hence, a skilled labor of sand casting, fully equipped with an appropriate instrumentation and data acquisition and control system, was employed. The test sample was a rectangular plate of Al-Si_5-Cu_3 aluminum alloy with dimensions 75×75×20 mm^3, shown in Fig.2. The experimentation procedure and setup were conducted at Sharp Technocast Industries, located in Kathwada GIDC, Ahmedabad.

Table IV
CASTING POROSITY VALUES AND S/N RATIO FOR DIFFERENT TRIALS

Exp. No.	Trial 1	Trial 2	Trial 3	Average	S/N Ratio
1	0.65	0.70	0.71	0.69	3.24
2	0.59	0.59	0.59	0.59	4.62
3	0.52	0.55	0.56	0.54	5.34
4	0.57	0.54	0.53	0.54	5.31
5	0.53	0.54	0.55	0.54	5.35
6	0.61	0.59	0.58	0.59	4.58
7	0.55	0.57	0.58	0.56	4.97
8	0.63	0.59	0.58	0.60	4.43
9	0.60	0.60	0.60	0.60	4.42
10	0.66	0.66	0.66	0.66	3.62
11	0.59	0.62	0.63	0.61	4.30
12	0.51	0.56	0.58	0.55	5.16
13	0.46	0.44	0.43	0.44	7.06
14	0.42	0.44	0.44	0.43	7.30
15	0.51	0.47	0.46	0.48	6.42
16	0.46	0.48	0.49	0.48	6.45
17	0.56	0.53	0.52	0.53	5.44
18	0.47	0.51	0.52	0.50	5.99
19	0.53	0.51	0.51	0.52	5.73
20	0.47	0.47	0.47	0.47	6.58
21	0.56	0.54	0.54	0.55	5.21
22	0.54	0.55	0.55	0.55	5.25
23	0.48	0.53	0.55	0.52	5.64
24	0.46	0.43	0.42	0.43	7.24
25	0.45	0.44	0.44	0.45	7.00
26	0.50	0.51	0.52	0.51	5.81
27	0.50	0.48	0.48	0.49	6.22

The system measures by means of sensors the values of the considered green-sand casting process parameters (thermocouples, velocity sensors, pressure sensors). Chromel/alumel thermocouples were used for temperature measurements.

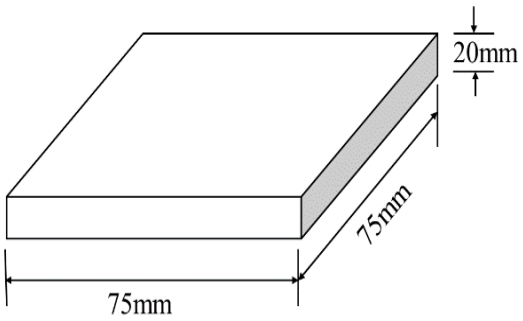

Table III
CHEMICAL COMPOSITION % OF GRADE $AlSi_5Cu_3$

Fe	max 0.6	**Ti**	max 0.25	**Zn**	max 0.2
Si	4.5 - 6	**Cu**	2.6 - 3.6	**Sn**	max 0.05
Mn	max 0.55	**Pb**	max 0.1	**Others**	each 0.05; total 0.15
Ni	max 0.1	**Mg**	max 0.05	**Remain**	Al

Fig. 2 Schematic diagram of the rectangular plate cast for experiment

Two thermocouples have been placed in each moulding box half at 50mm intervals along the casting centerline. For each trial condition, three castings were made using a randomization technique. The casting density was measured using the immersion technique. Castings were weighted first in air and then were immersed in thoroughly degassed distilled water. All weightings were conducted on a Mettler balance accurate to 0.0001 g. Porosity was calculated from the relationship below. where ρs is the measured casting density and ρ0 is the density of a fully dense casting having no porosity (2.75 kg/m^3).

$$Porosity(\%) = \left(1 - \frac{\rho_s}{\rho_0}\right) \times 100$$

In traditional experimental analysis, data primarily focuses on examining the mean response. However, the Taguchi method places emphasis on investigating both the mean response and response variation, employing the signal-to-noise (S/N) ratio. This approach aims to minimize variations in quality characteristics attributed to uncontrollable parameters [16,18,22]. Porosity, being a quality characteristic of the 'the smaller the better' type, is particularly pertinent in this context.

IV. Result And Discussion

Average values of porosity and the direct effects of various process parameters on porosity shown on table V. Each row represents a different combination of process parameters or their interactions, and the columns show the average values of porosity for each combination as well as the direct effects of the parameters. Table V explains process parameters which are denoted by letters A, B, C, D, and E. Average values of each parameter or interaction have three values corresponding to levels L_1, L_2, and L_3. Main effects values indicate the direct effect of changing the process parameter from one level to another. For example, "L_2-L_1" shows the effect of changing the parameter from level 1 to level 2, and similarly for other comparisons.

Process Parameters	**Average Values**			**Main Effects**		
	L_1	**L_2**	**L_3**	**L_2-L_1**	**L_3-L_2**	**L_3-L_1**
A	0.584	0.520	0.498	-0.063	-0.022	-0.086
B	0.574	0.503	0.525	-0.071	0.022	-0.050
A X B	0.537	0.549	0.517	0.012	-0.032	-0.020
A X B^2	0.513	0.524	0.565	0.011	0.041	0.052
C	0.542	0.534	0.526	-0.009	-0.008	-0.017
A X C	0.536	0.531	0.535	-0.006	0.004	-0.001
A X C^2	0.538	0.530	0.535	-0.008	0.005	-0.003
B X C	0.557	0.532	0.513	-0.025	-0.019	-0.043
D	0.538	0.546	0.518	0.009	-0.028	-0.020
E	0.550	0.517	0.535	-0.033	0.019	-0.014
B X C^2	0.550	0.517	0.535	-0.033	0.018	-0.014

For instance, taking parameter A, at level L_1, the average porosity is 0.584, at level L_2, the average porosity decreases to 0.520, resulting in a direct effect of -0.063. At level L3, the average porosity further decreases to 0.498, resulting in a direct effect of -0.086. Similarly, for parameter B, changing from level 1 to level 2 results in a decrease in porosity by 0.071 units, from level 2 to level 3 results in an increase in porosity by 0.022 units and changing from level 1 to level 3 results in a decrease in porosity by 0.050 units. The interactions between parameters, denoted by combinations like A X B, represent how the joint influence of two parameters affects porosity. For instance, the interaction A X B^2 shows that when both A and B are at their second levels, the average porosity increases to 0.565, with a direct effect of 0.052 compared to when only one of them is at level 2.

$$\text{S\N Ratio (dB)} = -10\log\left(1/n \sum_{i=1}^{n} Di^2\right)$$

The signal-to-noise ratio (S/N ratio) was employed to evaluate that specific type of response. It's calculated using the response value (Di) observed across a series of n repeated trials.

Next, S/N ratios were calculated for each of the 27 trial conditions. Table IV displays the resulting values, alongside the average of each parameter across different levels and the corresponding S/N ratios for each trial. The average casting porosity values for each parameter across levels 1 to 3 are tabulated in Table V and visualized in Figures 3 and 4. Additionally, Table V presents the main effects of the parameters as they transition from lower to higher levels.

If we look at table VI it explains at level L_1, the average S/N ratio is 4.696, at level L_2, the average S/N ratio increases to 5.749, resulting in a direct effect of 1.054. At level L_3, the average S/N ratio further increases to 6.076, resulting in a direct effect of 1.381. Similarly, for parameter B changing from level 1 to level 2 results in an increase in the S/N ratio by 1.149 units, from level 2 to level 3 results in a decrease in the S/N ratio by 0.376 units and changing from level 1 to level 3 results in an increase in the S/N ratio by 0.773 units. The interactions between parameters, denoted by combinations like A X B, represent how the joint

influence of two parameters affects the S/N ratio. For instance, the interaction A X B^2 shows that when both A and B are at their second levels, the average S/N ratio decreases to 5.005, with a direct effect of -0.885 compared to when only one of them is at level 2.

The average S/N ratios of process parameters on casting porosity at the different levels are given in Table VI and plotted in Fig. 5 & 6. Based on the analysis presented in Figures 3 and 4, it is evident that parameter E exhibits a higher degree of prominence compared to the other parameters under consideration.

Table VI
AVERAGE VALUES OF S\N RATIO AND DIRECT EFFECT OF PROCESS PARAMETER

Process Parameters	**Average Values**				**Main Effects**		
	L_1	**L_2**	**L_3**		**L_2-L_1**	**L_3-L_2**	**L_3-L_1**
A	4.696	5.749	6.076		1.054	0.327	1.381
B	4.867	6.015	5.639		1.149	-0.376	0.773
A X B	5.469	5.261	5.791		-0.208	0.530	0.322
A X B^2	5.890	5.626	5.005		-0.264	-0.621	-0.885
C	5.405	5.498	5.619		0.093	0.122	0.214
A X C	5.458	5.578	5.485		0.121	-0.093	0.028
A X C^2	5.471	5.550	5.500		0.079	-0.050	0.029
B X C	5.169	5.528	5.825		0.359	0.297	0.656
D	5.468	5.299	5.755		-0.169	0.456	0.287
E	5.274	5.783	5.465		0.509	-0.318	0.191
B X C^2	5.279	5.796	5.446		0.517	-0.350	0.167

Specifically, in Figure 3, the observed casting porosity reaches its minimum value when parameter A, B, C, and E are set at the third level, and parameter D is set at the first level. Moreover, the S/N ratio analysis (Fig. 4) suggests that the parameter levels A3, B3, C3, D1 and E3 are the best levels for reducing the green-sand casting porosity process variability of Al-Si_5-Cu_3 aluminum alloy. It must be noted that the above combination of factorial levels (3, 3, 3, 1, 3) was not one of the 27 combinations tested in the experimentation. This was expected because of the high fractionality in the employed experimental design (27 from 3^5 = 243 possible combinations).

A. Taguchi Analysis: Average, S/N Ratio Versus A, B, C, D, E

Taguchi analysis is a statistical method used for improving the quality of manufactured goods and processes. It involves designing experiments to optimize the performance characteristics of a product or process. One of the key components of Taguchi analysis is the Signal-to-Noise (S/N) ratio, which is used to assess the quality of a product or process. In Taguchi analysis, the goal is often to maximize the S/N ratio, as it represents the ratio of the signal (desired output) to the noise (undesired variation). Table VII and Table VIII represent response tables for Signal-to-Noise ratios (Table VII) and porosities (Table VIII). In Taguchi analysis, smaller values are generally preferred for both the S/N ratio (indicating less noise) and porosity (indicating better quality). Each table shows the average values of the response variable at different levels of the factors A, B, C, D, and E. Factor A has the highest impact on the S/N ratio, with a delta of 2.23, indicating significant variation across its levels. Factor B has the second-highest impact, followed by factors E, D, and C. Factor A again has the highest impact on porosity, with a delta of 0.648. Factor B has the second-highest impact, followed by factors E, D, and C.

Table VII
RESPONSE TABLE FOR SIGNAL TO NOISE RATIOS
(SMALLER IS BETTER)

Level	**A**	**B**	**C**	**D**	**E**
1	-10.41	-10.62	-11.44	-11.57	-11.26
2	-12.03	-12.50	-11.72	-11.38	-12.15
3	-12.64	-11.96	-11.92	-12.13	-11.67
Delta	2.23	1.88	0.49	0.75	0.89
Rank	1	2	5	4	3

Table VIII
RESPONSE TABLE FOR POROSITIES
(SMALLER IS BETTER)

Level	**A**	**B**	**C**	**D**	**E**
1	2.640	2.721	2.974	3.003	2.912
2	3.135	3.259	3.016	2.923	3.150
3	3.287	3.082	3.073	3.136	3.000
Delta	0.648	0.539	0.099	0.214	0.238
Rank	1	2	5	4	3

Table XII
ANOVA FOR AVERAGE POROSITY AND S/N RATIO

		Average Porosity				S/N Ratio			
Source	**DoF**	**Adj SS**	**Adj MS**	**F-Value**	**P-Value**	**Adj SS**	**Adj MS**	**F-Value**	**P-Value**
C	2	0.004693	0.002346	1.12	0.351	1.2847	0.6423	1.19	0.330
B	2	0.024179	0.012089	5.76	0.013	6.1759	3.0879	5.72	0.013
A	2	0.035550	0.017775	8.47	0.003	9.3691	4.6846	8.67	0.003
D	2	0.013618	0.006809	3.25	0.066	3.7192	1.8596	3.44	0.057
E	2	0.001230	0.000615	0.29	0.750	0.2079	0.1040	0.19	0.827
		Average Porosity							
Error	16	0.033569	0.002098			16	8.6422	0.5401	
Total	26	0.112838				26	29.3989		

For the value of B we can summaries that F-Value of 5.76 with a P-Value of 0.013 indicates that the parameter B is statistically significant in explaining the variation in both Average Porosity and S/N Ratio. Similarly for the process parameter A the F-Value of 8.47 with a P-Value of 0.003 suggests that the variable A is statistically significant in explaining the variation in both Average Porosity and S/N Ratio. For D it elaborates F-Value of 3.25 with a P-Value of 0.066 suggests that the variable D is marginally statistically significant (borderline) in explaining the variation in both Average Porosity and S/N Ratio. While E has the F-Value of 0.29 with a P-Value of 0.750 indicates that the variable E is not statistically significant in explaining the variation in both Average Porosity and S/N Ratio.

Table XIII
MODELS SUMMARY

	S	R-sq	R-sq(adj)	R-sq(pred)
Average Porosity	0.0458044	70.25%	51.66%	15.28%
S/N Ratio	0.734940	70.60%	52.23%	16.29%

Table XIV
MODEL SUMMARY

S	R-sq	R-sq(adj)	R-sq(pred)
0.0432405	70.17%	56.92%	28.25%

Best Fitted Observations

Obs	Average	Fit	Resid	Std Resid
1	0.6879	0.6130	0.0749	2.21

The Error term represents the unexplained variation in the data. The Total row shows the total variation in the data. These values are important for assessing the overall fit of the model. In summary, variables B and A appear to be statistically significant in explaining the variation in both Average Porosity and S/N Ratio, while variables C, D, and E, are either not significant or marginally significant. Finally, from the model summary (table XIII), we can interpret that model explains 70.25% of the variance in average porosity, after adjusting for the number of predictors, the adjusted R-squared is 51.66%. The model's predictive capability for new data, as indicated by the R-squared for Prediction, is 15.28%. The model explains 70.60% of the variance in S/N Ratio. After adjusting for the number of predictors, the adjusted R-squared is 52.23%. The model's predictive capability for new data, as indicated by the R-squared for Prediction, is 16.29%. The model appears to have moderate explanatory power (as indicated by R-squared and adjusted R-squared), with some ability to predict new data. Observation 1 has a higher-than-expected S/N Ratio compared to the model's prediction, suggesting it may be an outlier or an unusual observation.

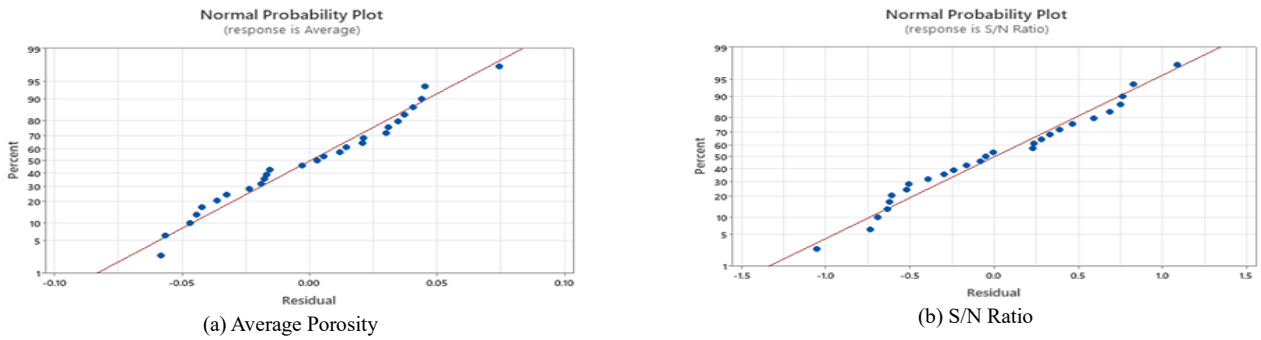

(a) Average Porosity (b) S/N Ratio

Figure 7 : Curve fitting for response variables (a) and (b) (Normalized P-P Plot for regression standardized residual dependent variables (a) and (b))

E. Regression Equations

Average porosity = 0.53407 + 0.0024 C_100 + 0.0148 C_250 - 0.0172 C_400 + 0.0404 B_10 - 0.0311 B_12- 0.0093 B_15 + 0.0497 A_710 - 0.0138 A_725 - 0.0359 A_740 - 0.0213 D_1.4 - 0.0098 D_2.6 + 0.0311 D_3.8 + 0.0084 E_180 - 0.0002 E_225- 0.0082 E_270

S/N ratio = 5.507 - 0.038 C_100 - 0.246 C_250 + 0.284 C_400 - 0.641 B_10 + 0.508 B_12 + 0.132 B_15- 0.811 A_710+ 0.242 A_725+ 0.569 A_740+ 0.383 D_1.4+ 0.119 D_2.6- 0.502 D_3.8- 0.102 E_180- 0.010 E_225 + 0.112 E_270 (Equation treats random terms as though they are fixed).

The regression equation for Average Porosity and the S/N Ratio is formulated, establishing a relationship between the intercept and the independent variables A, B, C, D, and E, along with their respective levels. This equation is graphically represented in Figure 7, illustrating the fitted curve for the response variables.

V. CONCLUSIONS

The porosity determination by the Taguchi method has been carried out in this study. As a part of the analysis of variance (ANOVA) conducted for both Average Porosity and S/N Ratio within the framework of the Taguchi method of optimization yields insightful conclusions for different parameters are (1) Volume hold in crucible C: The F-Value of 1.12, coupled with a P-Value of 0.351, indicates that parameter C is not statistically significant in explaining the variation in either Average Porosity or S/N Ratio. (2) Pouring time B: A significant finding emerges with an F-Value of 5.76 and a corresponding P-Value of 0.013, suggesting that parameter B significantly influences both Average Porosity and S/N Ratio. (3) Pouring temperature, A: Similarly, parameter A demonstrates statistical significance, as evidenced by an F-Value of 8.47 and a low P-Value of 0.003, indicating its influential role in explaining the variation in both Average Porosity and S/N Ratio. (4) Degassing time D: While parameter D exhibits a moderate F-Value of 3.25, its associated P-Value of 0.066 suggests marginal statistical significance, implying that it may play a borderline role in explaining the variation in both response variables. (5) Mould temperature E: In contrast, parameter E shows neither statistical significance nor influence on the variation in either Average Porosity or S/N Ratio, as evidenced by an F-Value of 0.29 and a high P-Value of 0.750.(6). The factors *A X B*, *A X C*, and *B X C* exert a considerable influence on the output, given their p-values are either less than 0.05 or close to it. The pouring temperature, pouring time, and volume in the crucible emerge as the most influential factors in green sand casting for porosity occurrence, as indicated by their p-values being less than 0.05 or approaching it.

The Error term signifies the unexplained variation in the data, while the Total row represents the entirety of variation present, both crucial for assessing the overall fit of the model. In summary, variables B and A emerge as statistically significant contributors to the variation in both response variables, while variables C, D, and E either lack significance or demonstrate marginal importance.

ACKNOWLEDGMENT

The author expresses heartfelt gratitude to M/S Sharp Technocast Industries, located at Kathwada GIDC, Ahmedabad, for their generous support for our research efforts. They provide essential facilities and expertise for execution of our experimentation and allowed us to conduct in-house experiments. We also acknowledged Mr. Sravankumar Jogunuri, Assistant professor, CAET, AAU, Godhra for his support and co-operation in derivation and evaluation of data to our crucial work.

REFERENCES

[1] B.R.T. Vilane, Assessment of stabilisation of adobes by confined compression tests. Biosyst Eng. 106.4 (2010) 551-558.

[2] T. Shanmugapriya, R.N. Uma, Optimization of partial replacement of m-sand by natural sand in high performance concrete with silica fume. Int. J. Eng. Sci. Emerg. Technol. 2.2 (2012) 73-80.

[3] Juran, J. M. Quality Control Handbook, 1979 (McGraw-Hill, New York).

[4] G.C.M. Patel, P. Krishna, M.B. Parappagoudar, Optimization of squeeze cast process parameters using Taguchi and grey relational analysis. Proc. Tech. 14 (2014) 157-164.

[5] P. Senthil, K.S. Amirthagadeswaran, Experimental study and squeeze casting process optimization for high quality AC2A aluminium alloy castings. Arab. J. Sci. Eng., 39.3 (2014) 2215- 2225.

[6] S. Kumar, P.S. Satsangi, D.R. Prajapati, Optimization of green sand casting process parameters of a foundry by using Taguchi's method. Int. J Adv. Manuf. Tech., 55.1-4 (2011) 23-34.

[7] G.R. Chate, G.C.M. Patel, R.M. Kulkarni, P. Vernekar, A.S. Deshpande, M.B. Parappagoudar, Study of the effect of nano-silica particles on resin-bonded moulding sand properties and quality of casting. Silicon (2018) 1-16.

[8] Kackar, R. N. Off-line quality control, parameter design and the Taguchi method. J. Qual. Technol., 1985, 17(4), 176–188.

[9] Logothetis, N. The role of data transformation in the Taguchi analysis. Quality and Reliability Engng Int., 1988, 4, 49–61.

[10] V.V. Reddy, P.M. Valli, A. Kumar, C.S. Reddy, Multi-objective optimization of electrical discharge machining of PH17-4 stainless steel with surfactant-mixed and graphite powder–mixed dielectric using Taguchi-data envelopment analysis–based ranking method. P I Mech. Eng. B-J Eng., 229.3 (2015). 487-494.

[11] T. Muthuramalingam, S. Vasanth, P. Vinothkumar, T. Geethapriyan, M.M. Rabik, Multi criteria decision making of abrasive flow oriented process parameters in abrasive water jet machining using Taguchi–DEAR methodology. Silicon (2018) 1-7.

[12] Phadke, S. M. Quality Engineering Using Robust Design,1989 (Prentice-Hall, Englewood Cliffs, New Jersey).

[13] B. Surekha, L.K. Kaushik, A.K. Panduy, P.R. Vundavilli, M.B. Parappagoudar, Multi-objective optimization of green sand mould system using evolutionary algorithms. Int. J Adv. Manuf. Tech., 58.1-4. (2012) 9-17.

[14] S.R. Pulivarti, A.K. Birru, Optimization of green sand mould system using Taguchi based grey relational analysis. China Foundry, 15.2 (2018)152-159.

[15] N.I.S. Hussein, M.N. Ayof, N.I. Mohamed Sokri, Mechanical properties and loss on ignition of phenolic and furan resin bonded sand casting. Int. J. Min. Met. Mech. Eng. 1(2013) 223-227.

[16] Taguchi, G. and Konishi, S. Orthogonal Arrays and Linear Graphs, 1987 (American Supplier Institute, Dearborn, Michigan).

[17] J.A. Ghani, I.A. Choudhury, H.H. Hassan, Application of Taguchi method in the optimization of end milling parameters, J. of Mat. Proc. Technol. 145 (2002) 84-92.

[18] Enright, T. P. and Price, B. Use of the Taguchi method for off-line quality control, parameter estimation and experimental design in the Casting Division of Ford Motor Company. AFS Trans., 1987, 87, 144–151.

[19] R.R. Kundu, B.N. Lahiri, Study and statistical modelling of green sand mould properties using RSM, Int. J. of Mat. nd Product Technol. 31 (2008) 143-158.

[20] C. Saikaew, S. Wiengwiset, Optimization of moulding sand composition for quality improvement of iron castings, Applied Clay Science 67-68 (2012) 26-31.

[21] S.N. Ramrattan, A.M. Paudel, H. Makino, M. Hirata, Desirable green sand properties via aeration sand filling, Transactions of the American Foundry Men's Society 116 (2008) 493-503.

[22] Dahle, A. K., Arnberg, L. and Apelian, D. Burst feeding and its role in porosity formation during solidification of Al foundry alloys. AFS Trans., 1997, 160, 963–969.

[23] Chiesa, F., Fuoco, R. and Gruzleski, J. E. Porosity distribution in directionally solidified test bars sand cast from a controlled A356 melt. Int. J. Cast Metals, 1995, 7(2), 113– 122.

[24] B. H. Kim, J. S. Shin, S. M Lee, B. M. Moon: Improvement of tensile strength and corrosion resistance of highsilicon cast irons by optimizing casting process parameters, J Mater Sci (2007) 42:109- 117.

[25] Ballal Yuvraj P., Dr. Inamdar K. H., Patil P. V.: Application of Taguchi method for design of experiments in turning gray cast iron. International Journal of Engineering Research and Applications (IJERA) Vol. 2, Issue 3, May-Jun 2012, pp. 1391-1397.

[26] V. D Tsoukalas, St A Mavrommatis, N G Orfanoudakis and A K Baldoukas, " A study of porosity formation in pressure die casting using the Taguchi approach", Proc. Instn Mech. Engrs. Vol. 218 Part B: J. Engineering Manufacture 2004.

[27] A. Noorul Haq, S. Guharaja, K. M. Karuppannan: Parameter optimization of CO2 casting process by using Taguchi method. Int J Interact Des Manuf (2009) 3:41-50

[28] Sushil Kumar, P. S. Satsangi, D. R. Prajapati: Optimization of green sand casting process parameters of a foundry using Taguchi's method, Int J Adv. Manu f Technology (2011) 55:23 – 34.

[29] M. Perzyk and A. Kochanski, Detection of Causes of Casting Defects Assisted by Artificial Neural Networks, Institute of Materials Processing, Warsaw University of Technology, Warsaw, Poland, 2003, vol. 217, pp.1279-1284.

[30] Rahul Bhedasgaonkar, Uday A. Dabade, May 2012, Analysis of Casting Defects by Design of Experiments Method, Proceedings of 27th National Convention of Production Engineers and National Seminar on Advancements in Manufacturing – VISION 2020, organized by BIT, Mesra, Ranchi, India

[31] W. M. Abu Jadayi, "Studying the effects of varying the pouring rate on the casting defects using nondestructive testing techniques," *Jordan J. Mech. Ind. Eng.*, vol. 5, no. 6, pp. 521–526, 2011.

[32] A. Sharma and A. K. Sinha, "Ultrasonic Testing for Mechanical Engineering Domain: Present and Future Perspective," vol. 7, no. 2, pp. 243–253, 2018, doi: 10.22105/riej.2018.100730.1018.

[33] J. Idris and A. Al-bakoosh, "Akademia Baru Application of Non-Destructive Testing Techniques for the Assessment of Casting of AA5083 Alloy Akademia Baru," vol. 3, no. 1, pp. 25–34, 2014.

[34] J. Lin, Y. Yao, L. Ma, and Y. Wang, "Detection of a casting defect tracked by deep convolution neural network," *Int. J. Adv. Manuf. Technol.*, vol. 97, no. 1–4, pp. 573–581, 2018, doi: 10.1007/s00170-018-1894-0.

[35] W. Du, H. Shen, J. Fu, G. Zhang, and Q. He, "Approaches for improvement of the X-ray image defect detection of automobile casting aluminum parts based on deep learning," *NDT E Int.*, vol. 107, no. May, p. 102144, 2019, doi: 10.1016/j.ndteint.2019.102144.

[36] A. B. H. Bejaxhin, G. Paulraj, and M. Prabhakar, "Inspection of casting defects and grain boundary strengthening on stressed Al6061 specimen by NDT method and SEM micrographs," *J. Mater. Res. Technol.*, vol. 8, no. 3, pp. 2674–2684, 2019, doi: 10.1016/j.jmrt.2019.01.029.

[37] S. Mozammil, J. Karloopia, and P. K. Jha, "Investigation of porosity in Al casting," *Mater. Today Proc.*, vol. 5, no. 9, pp. 17270–17276, 2018, doi: 10.1016/j.matpr.2018.04.138.

[38] A. I. Cheprasov, S. V. Knyazev, A. A. Usoltsev, A. E. Dolgopolov, and R. O. Mamedov, "Detection of cold cracks in the cast-steels by the methods of ultrasonic and eddy-current infrared thermography," *IOP Conf. Ser. Mater. Sci. Eng.*, vol. 150, no. 1, 2016, doi: 10.1088/1757-899X/150/1/012026.

[39] C. Jin, X. Kong, J. Chang, H. Cheng, and X. Liu, "Internal crack detection of castings: a study based on relief algorithm and Adaboost-SVM," *Int. J. Adv. Manuf. Technol.*, vol. 108, no. 9–10, pp. 3313–3322, 2020, doi: 10.1007/s00170-020-05368-w.

[40] M. Ferguson, R. Ak, Y.-T. T. Lee, and K. H. Law, "Automatic localization of casting defects with convolutional neural networks," pp. 1726–1735, 2018, doi: 10.1109/bigdata.2017.8258115.

[41] W. Du, H. Shen, J. Fu, G. Zhang, X. Shi, and Q. He, "Automated detection of defects with low semantic information in X-ray images based on deep learning," *J. Intell. Manuf.*, 2020, doi: 10.1007/s10845-020-01566-1.

[42] E. Hanks, D. Liu, and A. Palazotto, "Surface roughness of electron beam melting Ti-6Al-4v effect on ultrasonic testing," *57th AIAA/ASCE/AHS/ASC Struct. Struct. Dyn. Mater. Conf.*, no. January, pp. 1–13, 2016, doi: 10.2514/6.2016-1512.

[43] I. Narasimha Murthy and J. Babu Rao, "Non Destructive Evaluation of A356 alloy Castings made in Sand and Granulated Blast Furnace Slag Moulds," *Mater. Today Proc.*, vol. 5, no. 1, pp. 168–174, 2018, doi: 10.1016/j.matpr.2017.11.068.

[44] S. A. Arhamnamazi, N. B. M. Arab, A. R. Oskouei, and F. Aymerich, "Accuracy assessment of ultrasonic C-scan and X-ray radiography methods for impact damage detection in glass fiber reinforced polyester composites," *J. Appl. Comput. Mech.*, vol. 5, no. 2, pp. 258–268, 2019, doi: 10.22055/JACM.2018.26297.1318.

[45] S. A. Patil and P. D. Darade, "Application and Performance Frequency Response Method as NDT Tool to Detect Defects in Castings," *Mater. Today Proc.*, vol. 4, no. 8, pp. 8463–8468, 2017, doi: 10.1016/j.matpr.2017.07.192.

[46] B. R. Goodlet, L. H. Rettberg, and T. M. Pollock, "Resonant ultrasound spectroscopy for defect detection in single crystal superalloy castings," *Proc. Int. Symp. Superalloys*, vol. 2016-Janua, no. October, pp. 303–312, 2016, doi: 10.1002/9781119075646.ch33.

[47] W. Orłowicz, M. Tupaj, M. Mróz, and E. Guzik, "Evaluation of ductile iron casting material quality using ultrasonic testing," *J. Mater. Process. Technol.*, vol. 210, no. 11, pp. 1493–1500, 2010, doi: 10.1016/j.jmatprotec.2010.04.007.

[48] A. Messager *et al.*, "In situ synchrotron ultrasonic fatigue testing device for 3D characterisation of internal crack initiation and growth," *Fatigue Fract. Eng. Mater. Struct.*, vol. 43, no. 3, pp. 558–567, 2020, doi: 10.1111/ffe.13140.

[49] C. Brugger, T. Palin-Luc, P. Osmond, and M. Blanc, "A new ultrasonic fatigue testing device for biaxial bending in the gigacycle regime," *Int. J. Fatigue*, vol. 100, pp. 619–626, 2017, doi: 10.1016/j.ijfatigue.2016.12.039.

[50] A. Chabot, N. Laroche, E. Carcreff, M. Rauch, and J. Y. Hascoët, "Towards defect monitoring for metallic additive manufacturing components using phased array ultrasonic testing," *J. Intell. Manuf.*, vol. 31, no. 5, pp. 1191–1201, 2020, doi: 10.1007/s10845-019-01505-9.

[51] A. Moghanizadeh, "Evaluation of the physical properties of spot welding using ultrasonic testing," *Int. J. Adv. Manuf. Technol.*, vol. 85, no. 1–4, pp. 535–545, 2016, doi: 10.1007/s00170-015-7952-y.

[52] R. Wang, Z. Liu, J. Wu, B. Jiang, and B. Li, "Research on phased array ultrasonic testing on CFETR vacuum vessel welding," *Fusion Eng. Des.*, vol. 139, no. January, pp. 124–127, 2019, doi: 10.1016/j.fusengdes.2019.01.050.

[53] G. Raju and M. Ashok, "The Phased Array Advantage of Ultrasonic Scanning of Rocket Motor Cases of Indian Satellite Launch Vehicles," no. December, pp. 14–16, 2017.

[54] J. Parra-Raad, P. Khalili, and F. Cegla, "Shear waves with orthogonal polarisations for thickness measurement and crack detection using EMATs," *NDT E Int.*, vol. 111, p. 102212, 2020, doi: 10.1016/j.ndteint.2019.102212.

[55] A. Maurer, W. Deodorico, R. Huber, and T. Laffont, "Aerospace Composite Testing Solutions using Industrial Robots," *18th World Conf. Nondestruct. Test.*, no. April, p. 7, 2012, [Online]. Available: https://www.ndt.net/article/wcndt2012/papers/166_wcndtfinal00166.pdf.

[56] P. Khalili and P. Cawley, "The choice of ultrasonic inspection method for the detection of corrosion at inaccessible locations," *NDT E Int.*, vol. 99, no. June, pp. 80–92, 2018, doi: 10.1016/j.ndteint.2018.06.003.

[57] S. Palanisamy, C. R. Nagarajah, and P. Iovenitti, "Ultrasonic inspection of rough surface aluminium die castings," *Insight Non-Destructive Test. Cond. Monit.*, vol. 49, no. 3, pp. 160–164, 2007, doi: 10.1784/insi.2007.49.3.160.

[58] S. nan Xue, Q. chi Le, Y. hui Jia, L. ping Jiang, Z. qiang Zhang, and L. Bao, "Ultrasonic flaw detection of discontinuous defects in magnesium alloy materials," *China Foundry*, vol. 16, no. 4, pp. 256–261, 2019, doi: 10.1007/s41230-019-9041-6.

[59] I. Baillie, P. Griffith, X. Jian, and S. Dixon, "Implementing an ultrasonic inspection system to find surface and internal defects in hot, moving steel using E18MATs," *AIP Conf. Proc.*, vol. 1096, no. 2, pp. 1711–1718, 2009, doi: 10.1063/1.3114165.

[60] D. M. Schwabe, A. Maurer, and R. Koch, "Ultrasonic Testing Machines with Robot Mechanics – A New Approach to CFRP Component Testing," *Aerospace*, pp. 1–5, 2010.

[61] C. Garnier, M. L. Pastor, F. Eyma, and B. Lorrain, "The detection of aeronautical defects in situ on composite structures using non destructive testing," *Compos. Struct.*, vol. 93, no. 5, pp. 1328–1336, 2011, doi: 10.1016/j.compstruct.2010.10.017.

[62] R. A. Smith, L. J. Nelson, M. J. Mienczakowski, and R. E. Challis, "Automated analysis and advanced defect characterisation from ultrasonic scans of composites," *Insight Non-Destructive Test. Cond. Monit.*, vol. 51, no. 2, pp. 82–87, 2009, doi: 10.1784/insi.2009.51.2.82.

[63] A. Habibalahi, M. D. Moghari, K. Samadian, S. S. Mousavi, and M. S. Safizadeh, "Improving pulse eddy current and ultrasonic testing stress measurement accuracy using neural network data fusion," *IET Sci. Meas. Technol.*, vol. 9, no. 4, pp. 514–521, 2015, doi: 10.1049/iet-smt.2014.0211.

[64] S. Roccella *et al.*, "Development of an ultrasonic test method for the non-destructive examination of ITER divertor components," *Fusion Eng. Des.*, vol. 84, no. 7–11, pp. 1639–1644, 2009, doi: 10.1016/j.fusengdes.2008.12.096.

[65] A. Kumar, C. J. Torbet, T. M. Pollock, and J. Wayne Jones, "In situ characterization of fatigue damage evolution in a cast Al alloy via nonlinear ultrasonic measurements," *Acta Mater.*, vol. 58, no. 6, pp. 2143–2154, 2010, doi: 10.1016/j.actamat.2009.11.055.

[66] H. Kato, T. Suzuki, Y. Annou, and K. Kageyama, "Nondestructive detection of cold flakes in aluminum alloy die-cast plate with ultrasonic measurement," *Mater. Trans.*, vol. 45, no. 7, pp. 2403–2409, 2004, doi: 10.2320/matertrans.45.2403.

[67] Q. Y. Lu and C. H. Wong, "Applications of non-destructive testing techniques for post-process control of additively manufactured parts," *Virtual Phys. Prototyp.*, vol. 12, no. 4, pp. 301–321, 2017, doi: 10.1080/17452759.2017.1357319.

[68] E. Ayorinde *et al.*, "Reliable low-cost NDE of composite marine sandwich structures," *Compos. Part B Eng.*, vol. 39, no. 1, pp. 226–241, 2008, doi: 10.1016/j.compositesb.2007.02.028.

[69] E. Jasiūnienė *et al.*, "Ultrasonic NDT of wind turbine blades using contact pulse-echo immersion testing with moving water container," *Ultragarsas (Ultrasound)*, vol. 63, no. 3, pp. 28–32, 2008, doi: 10.5755/J01.U.63.3.17075.

[70] A. Wilczek, P. Długosz, and M. Hebda, "Porosity Characterization of Aluminium Castings by Using Particular Non-destructive Techniques," *J. Nondestruct. Eval.*, vol. 34, no. 3, pp. 1–7, 2015, doi: 10.1007/s10921-015-0302-z.

[71] I. Amenabar, A. Mendikute, A. López-Arraiza, M. Lizaranzu, and J. Aurrekoetxea, "Comparison and analysis of non-destructive testing techniques suitable for delamination inspection in wind turbine blades," *Compos. Part B Eng.*, vol. 42, no. 5, pp. 1298–1305, 2011, doi: 10.1016/j.compositesb.2011.01.025.

[72] X. E. Gros, J. Bousigue, and K. Takahashi, "NDT data fusion at pixel level," *NDT E Int.*, vol. 32, no. 5, pp. 283–292, 1999, doi: 10.1016/S0963-8695(98)00056-5.

[73] T. Hasiotis, E. Badogiannis, and N. G. Tsouvalis, "Application of ultrasonic C-scan techniques for tracing defects in laminated composite materials," *Stroj. Vestnik/Journal Mech. Eng.*, vol. 57, no. 3, pp. 192–203, 2011, doi: 10.5545/sv-jme.2010.170.

[74] L. Nastac, M. N. Gungor, I. Ucok, K. L. Klug, and W. T. Tack, "Advances in investment casting of Ti – 6Al – 4V alloy : a review," vol. 19, no. 2, pp. 73–93, 2006, doi: 10.1179/136404605225023225.

[75] S. Liu and Y. C. Shin, "Additive manufacturing of Ti6Al4V alloy : A review," *Mater. Des.*, vol. 164, p. 107552, 2019, doi: 10.1016/j.matdes.2018.107552.

[76] S. Gholizadeh, "ScienceDirect ScienceDirect ScienceDirect A review of non-destructive testing methods of composite materials Thermo-mechanical modeling of a high pressure turbine blade of an airplane gas turbine engine," *Procedia Struct. Integr.*, vol. 1, pp. 50–57, 2016, doi: 10.1016/j.prostr.2016.02.008.

[77] S. Kumar, M. Vishwakarma, and P. Akhilesh, "ScienceDirect Advances and Researches on Non Destructive Testing : A Review," vol. 5, pp. 3690–3698, 2018.

[78] P. Tao, H. Shao, Z. Ji, H. Nan, and Q. Xu, "Numerical simulation for the investment casting process of a large-size titanium alloy thin-wall casing," *Prog. Nat. Sci. Mater. Int.*, vol. 28, no. 4, pp. 520–528, 2018, doi: 10.1016/j.pnsc.2018.06.005.

[79] H. Huaishu, Y. Xiao Dong, L. Ding, F. Xinchong, and S. Jicai, "Detection and Analysis of Metal Induction Hardened Layer Based on Ultrasonic Technology," *J. Phys. Conf. Ser.*, vol. 1965, no. 1, pp. 5–9, 2021, doi: 10.1088/1742-6596/1965/1/012146.

[80] F. Honarvar and A. Varvani-Farahani, "A review of ultrasonic testing applications in additive manufacturing: Defect evaluation, material characterization, and process control," *Ultrasonics*, vol. 108, no. February, p. 106227, 2020, doi: 10.1016/j.ultras.2020.106227.

[81] H. Chen, M. Liu, Z. Hu, M. Li, and S. Li, "Mechanical structural health prognosis with nonlinear mixed frequency ultrasonic signal analysis," vol. 01075, pp. 1–10, 2021.

[82] R. Ahmad, N. A. Talib, and M. B. A. Asmael, "Effect of pouring temperature on microstructure properties of Al-Si LM6 alloy sand casting," *Appl. Mech. Mater.*, vol. 315, no. June, pp. 856–860, 2013, doi: 10.4028/www.scientific.net/AMM.315.856.